A small molecule mimicking a phosphatidylinositol (4,5)-bisphosphate binding pleckstrin homology domain

[1,2]Lok Hang Mak, [1]Savvas N. Georgiades, [2]Evelyn Rosivatz, [1,3]Gillian F. Whyte, [1]Marianna Mirabelli, [1,3]Ramon Vilar, [1,3]Rudiger Woscholski

[1]Department of Chemistry, Imperial College London, Exhibition Road, London SW7 2AZ, U.K.

[2]Division of Cell and Molecular Biology, Imperial College London, Exhibition Road, London SW7 2AZ, U.K.

[3]Institute of Chemical Biology, Imperial College London, Exhibition Road, London SW7 2AZ, U.K.

Corresponding author:

Dr Rudiger Woscholski

Email: r.woscholski@imperial.ac.uk

ABSTRACT

Inositol phospholipids have emerged as important key players in a wide variety of cellular functions. Among the seven existing inositol phospholipids, phosphatidylinositol (4,5)-bisphosphate ($PI(4,5)P_2$) has attracted much attention in recent years due to its important role in numerous cellular signaling events and regulations, which in turn impact several human diseases. This particular lipid is recognized in the cell by specific lipid binding domains, such as the Pleckstrin-homology (PH) domain, which is also employed as a tool to monitor this important lipid. Here, we describe the synthesis and biological characterization of a small molecule that mimics the PH domain as judged by its ability to bind specifically to only $PI(4,5)P_2$ and effectively compete with the PH domain *in vitro* and in a cellular environment. The binding constant of this small molecule PH domain mimetic (PHDM) was determined to be 17.6 ± 10.1 μM, similar in potency to the PH domain. Using NIH 3T3 mouse fibroblast cells we demonstrated that this compound is cell permeable and able to modulate $PI(4,5)P_2$-dependent effects in a cellular environment such as the endocytosis of the transferrin receptor, loss of mitochondria as well as stress fiber formation. This highly $PI(4,5)P_2$-specific chemical mimetic of a PH domain, is not only a powerful research tool, but might also be a lead compound in future drug developments targeting $PI(4,5)P_2$-dependent diseases such as Lowe syndrome.

INTRODUCTION

Phosphatidylinositol 4,5-bisphosphate ($PI(4,5)P_2$) is an important inositol phospholipid, since it is the precursor for several second messengers, such as phosphatidylinositol 3,4,5-trisphosphate (PIP_3) (*1*), diacylglycerol and 1,4,5-trisphosphate (IP_3) (*2*). In addition, $PI(4,5)P_2$ interacts with a variety of proteins such as profilin, gelsolin and α-actinin, which regulate the polymerization and depolymerization of actin in the cytoskeleton (*3, 4*). Recently, it has been demonstrated that $PI(4,5)P_2$ plays an important role in the processes of exocytosis and endocytosis as well as the regulation of a variety of ion channels (*5*), suggesting that $PI(4,5)P_2$ could be a key regulator of many cellular processes and diseases (*6*). Lowe syndrome for example, is caused by the mutation of the inositol-5-phosphatase OCRL, resulting in elevated $PI(4,5)P_2$ levels (*6,*).

Cellular levels of this lipid are maintained mainly by a balance between the phosphatidylinositol-monophosphate kinases (synthesis) and the counteracting phosphatidylinositol phosphatases (breakdown) (*8, 9*). Changes of $PI(4,5)P_2$ levels are detected by lipid binding proteins via lipid recognition domains such as the pleckstrin homology domain (PH domain), which possesses sub micro-molar affinity and specificity for $PI(4,5)P_2$ (*10*). For example, the PH domain of phospholipase C-δ1 selectively binds $PI(4,5)P_2$ and its head group IP_3, and thus has been applied as a tool to detect and image $PI(4,5)P_2$-levels (*11*). Furthermore, this PH domain has also been employed as a $PI(4,5)P_2$ sequestering tool causing a loss of available $PI(4,5)P_2$ levels. As demonstrated by Raucher et al. (*4*) overexpression of this PH domain resulted in the loss of actin stress fibers (cytoskeleton), an effect that could also be observed by overexpression of a $PI(4,5)P_2$ specific phosphatase. Thus, sequestering (PH domain binding) and removal (phosphatase) of cellular $PI(4,5)P_2$ affects cellular function in a similar fashion.

Chemical alternatives to alter cellular $PI(4,5)P_2$ concentrations do not really exist. Neomycin as well as poly-lysine have been proposed as tools to sequester cellular $PI(4,5)P_2$, but their use are restricted due to the lack of sufficient potency and selectivity (*12-14*), leaving a real void of chemical receptors that would be able to recognize a specific inositol phosphate in a cellular environment. We therefore set out to design a chemical receptor that would be able to do this. In this paper we present the development of such a receptor and detailed studies of its ability to bind $PI(4,5)P_2$ *in vitro* and *in vivo*. This is the first report on a small molecule able to recognize $PI(4,5)P_2$ displaying high affinity and specificity, effectively mimicking a PH domain.

RESULTS and DISCUSSION

Design and development of a chemical receptor for $PI(4,5)P_2$.

In order to design a specific chemical receptor for $PI(4,5)P_2$ that is capable of mimicking the efficacy of the equivalent biological tools (e.g. PH domain) unique recognition motifs in the targeted molecule have to be utilized. The head group of $PI(4,5)P_2$ contains phosphate and hydroxyl functionalities (see Figure 1a) that can be exploited for this purpose. For example, it is well established that ureas can form complementary hydrogen bonding interactions with phosphates (*15-18*), while boronic acids have been successfully used for the molecular recognition of diols via the reversible formation of B-O covalent bonds (*19, 20*). Thus, we designed a chemical receptor (PHDM) that utilizes ureas and boronic acids as recognition motifs (see Figure 1b). In this receptor, a large central spacer was employed with the aim of generating two recognition pockets (each containing a urea, secondary amine and a phenyl boronic acid group), which allows binding to two target molecules (see Figure 1c). This approach of a tandem receptor has been successfully used to increase specificity and affinity

of biological lipid recognition domains (*21*), a benefit desired for our chemical receptor designed here.

The $PI(4,5)P_2$ receptor PHDM was synthesized via the three-step process shown in Scheme 1. First, monoprotected amine **1** was reacted with 2-formylphenylboronic acid followed by reduction (with $NaBH_4$) of the resulting imine to yield compound **2**. This was followed by deprotection of the benzylamine to generate compound **3**, which was reacted with the 4,4'-methylenebis(phenyl isocyanate) to yield the bis-urea, bis-boronic acid target compound PHDM. The purity and integrity of PHDM was confirmed by ^{1}H and ^{13}C NMR spectroscopy, IR spectroscopy, mass spectrometry, HPLC separation (which showed only one trace) and elemental analyses (see Materials and Methods section).

PHDM binds $PI(4,5)P_2$

To demonstrate the ability of the PHDM to bind $PI(4,5)P_2$, we developed an enzyme-linked immunosorbant assay (ELISA) where we employed the PH domain of phospholipase C-δ1 (PLC-δ1) to detect the available $PI(4,5)P_2$ after exposure to increasing concentrations of PHDM (see Supplementary Figure 1). Since this assay provides a linear detection range in the presence of 80–500 nM PH domain (Figure 2b), the competition ELISA was performed with varying PHDM concentrations in the presence of 125 nM PH domain. As shown in Figure 2b, PHDM affects the binding of the PLC-δ1-PH domain to $PI(4,5)P_2$ already at very low concentrations (~3 μM) demonstrating high potency (K_d = ~18 μM).

PHDM inhibits PI(4,5)P_2 phosphatases

Next, we examined whether PHDM would be an effective inhibitor of PI(4,5)P_2 metabolizing enzymes, since adding PHDM would lower the effective substrate (PI(4,5)P_2) concentration. Thus, we tested the compound's potency on three different phosphoinositide phosphatases (SopB, OCRL and SKIP) that preferentially hydrolyze PI(4,5)P_2 (*22-26*).

As shown in Figures 3a–c, increasing concentrations of PHDM inhibit all tested phosphatases implying that the compound is binding PI(4,5)P_2 potently, effectively competing with the enzymes for their substrate. Interestingly, compound PHDM seems to be more potent on OCRL and SKIP phosphatases, although all three enzymes display similar K_M towards PI(4,5)P_2. However, this could be due to the wider substrate specificity of SopB, which also dephosphorylates the generated PI(4)P. To ensure that the observed reduction in phosphate release is not due to PHDM interacting with the enzyme, we employed 3-*O*-methylfluorescein phosphate (OMFP), an artificial substrate without any structural similarity to inositols. By employing this substrate any interaction of PHDM with the enzymes itself will become obvious, since the preferred target for PHDM, the substrate PI(4,5)P_2, will be missing. As shown in Figure 3d, no significant decrease in enzyme activity was detected in the presence of 50 μM PHDM as compared to the vehicle control. This proves that PHDM does not bind OMFP or the employed phosphatases SopB and SKIP. OCRL could not be tested in this manner, since it has no detectable OMFP activity. We therefore can conclude that the reduced phosphate release in the phosphatase assays is an effect of PHDM binding to the available PI(4,5)P_2 substrate and not due to interactions with the three tested enzymes.

Specificity of PHDM towards the head group of inositol lipids

Having confirmed that PHDM is capable of inhibiting $PI(4,5)P_2$ hydrolysis in phosphatase assays, we investigated the specificity of PHDM for different inositol phosphate head groups. Firstly, we tested PHDM's ability to interact with the soluble head group of its target $PI(4,5)P_2$, namely $I(1,4,5)P_3$. Previous studies have shown that the PLC-δ1 PH domain, the biological equivalent of PHDM, binds about 8-fold more strongly to the water soluble $I(1,4,5)P_3$ than $PI(4,5)P_2$ (*27*). To examine the binding affinity of PHDM to $I(1,4,5)P_3$ in comparison to $PI(4,5)P_2$, we made use of the phosphatase OCRL ability to hydrolyze $I(1,4,5)P_3$ as well as $PI(4,5)P_2$ (*25*). Surprisingly, although $I(1,4,5)P_3$ resembles the head group of $PI(4,5)P_2$, PHDM inhibits OCRL activity better when the lipid substrate is employed (see Figure 4a). This implies a stronger binding of PHDM to $PI(4,5)P_2$ than $I(1,4,5)P_3$,which is in contrast to the PLC-δ1 PH domain, where $I(1,4,5)P_3$ is clearly favored over $PI(4,5)P_2$. For comparison, PHDM was also tested for its ability to bind $PI(3,4,5)P_3$, which is generated *in vivo* by the action of PI 3-kinase on $PI(4,5)P_2$ (*1*). The balance of $PI(4,5)P_2$ and $PI(3,4,5)P_3$ is maintained by PTEN, which counteracts PI 3-kinase by de-phosphorylating $PI(3,4,5)P_3$ at the 3'-position (*28*). As shown in Figure 4a, PHDM was unable to influence PTEN's activity, indicating that PHDM does not bind $PI(3,4,5)P_3$ or PTEN. In order to investigate inositol phosphate isomers, all naturally occurring inositol-phospholipids were subjected to a SopB assay, since SopB is known to hydrolyze all these lipids (*22, 29*). As shown in Figure 4b, the hydrolysis of $PI(4,5)P_2$ by SopB is reduced in the presence of 50 μM PHDM to about 20% of the solvent (DMSO) control. Strikingly, all other PI-lipids were only minimally affected by PHDM, demonstrating that this compound has a much lower binding affinity for these related inositol phosphate head groups. Finally, we tested the ability of PHDM to compete with lipid-binding proteins commonly used to detect phosphoinositides. Therefore, we modified a protein-lipid overlay assay, which is generally used to study binding affinities between lipids

and PH domains (*30*). Normally, lipids are adsorbed onto blotting membranes, which are then probed with labeled proteins revealing their corresponding specificity. As shown in figure 4d, only the PI(4,5)P_2-binding PLC-δ1 PH domain was effectively blocked at low micromolar concentrations, with a complete loss of PH domain binding above 10 μM PHDM. Binding of the Akt PH domain towards PI(3,4)P_2 was only significantly affected at PHDM concentration of 50 μM, whereas the other lipid binding domains seem to be unaffected by up to 50 μM PHDM.

Compound PHDM binds to PI(4,5)P_2in NIH 3T3 mouse fibroblasts

Collectively, the data presented above clearly demonstrate that PHDM is a potent and specific PI(4,5)P_2-binding agent *in vitro*. In order to characterize the potency of PHDM in a cellular environment we first determined the cytotoxicity of PHDM on cells by using the MTT assay (*31*). As shown in Figure 5a, PHDM has no cytotoxic effect when fibroblast cells were treated for 2 h at concentrations as indicated. Even after prolonged exposure of 16 h, cell viability was still maintained at ~80% of vehicle control.

Having confirmed that PHDM is not cytotoxic to fibroblast cells, we next investigated the compound's ability to compete with the PLC-δ1 PH domain for PI(4,5)P_2 in a cellular environment (fixed cells). NIH 3T3 cells were treated with increasing concentrations of PHDM, fixed and subjected to PI(4,5)P_2 staining by employing the PLC-δ1 PH domain as a probe. As shown in Figure 5b, strong PI(4,5)P_2 staining can be observed in the vehicle (DMSO) control, with higher fluorescence intensity at the PI(4,5)P_2 rich plasma membrane (*32*). With increasing concentrations of PHDM, the PI(4,5)P_2 staining decreases (>5μM PHDM) almost abolishing PI(4,5)P_2 staining at concentrations above10 μM of PHDM. This

data demonstrate that PHDM is capable of crossing through cellular membranes (cell permeable), reaching the inside of the cell where it then binds cellular $PI(4,5)P_2$, effectively competing with the PH domain probe in a dose-dependent manner. In order to evaluate the PHDM's ability to compete with the PLC-δ1 PH domain *in vivo*, we employed cells over-expressing GFP labeled PLC-δ1 PH domains (see figure 5c). Increasing concentrations of PHDM correlated with increasing translocation of the PH domain (green) from the plasma membrane to the cytosol, with a complete loss of membrane localization achieved at PHDM concentrations higher than 30 μM. This process appears to start after 10 minutes of exposure to PHDM, being nearly completed within 30 minutes (see figure 5d). Taken together these data demonstrate the capability of PHDM to enter living cells, wherein this chemical $PI(4,5)P_2$ receptor displaces the natural $PI(4,5)P_2$ binding proteins (i.e. PLC-δ1 PH domain), which in turn suggests that PHDM is binding its intended target in living cells.

PHDM inhibits $PI(4,5)P_2$ dependant transferrin endocytosis

Having established that PHDM binds $PI(4,5)P_2$ *in vivo*, we investigated whether the PHDM-induced changes in free $PI(4,5)P_2$ levels would manifest in a changed cellular function.

$PI(4,5)P_2$ has been reported to regulate trafficking of numerous proteins to and from the plasma membrane that are required for receptor endocytosis such as the internalization of the transferrin receptor (*33*). Transferrin, an iron-binding glycoprotein, is transported into the cell by receptor-mediated endocytosis. However, depletion of plasma membrane $PI(4,5)P_2$ causes a severe inhibition of the uptake of transferrin in COS-7 cells (*33*). We therefore investigated the effect of PHDM on transferrin receptor uptake in a similar fashion. As shown in Figure 6a (top panel), FITC-conjugated transferrin was internalized and distributed in punctuated structure dispersed throughout the cytoplasm (yellow color). However, in the presence of

compound PHDM, the uptake of transferrin was drastically reduced (bottom panel; Figure 6a). These results demonstrate that PHDM inhibits the endocytosis of the transferrin receptor (Figure 6b), suggesting that it also blocks $PI(4,5)P_2$ dependent signaling and membrane traffic.

PHDM decreases the formation of long actin stress-fibers in fibroblast cells

Another cellular effector of $PI(4,5)P_2$ is the cytoskeleton, which is well known to interact directly with this lipid (*4*). In particular, increases in cellular $PI(4,5)P_2$ levels stimulate the formation of stress-fibers, whereas a loss of $PI(4,5)P_2$ leads to actin depolymerization (*3, 4*). There are three possible routes to deplete cellular $PI(4,5)P_2$: firstly, PLC-mediated hydrolysis to $I(1,4,5)P_3$ and DAG; secondly, hydrolysis to PI(4)P by inositol-5-phosphatases and finally conversion to $PI(3,4,5)P_3$ by PI 3-kinases. The latter pathway can be easily employed to disturb $PI(4,5)P_2$ levels by activating PI 3-kinases via growth factor stimulation (e.g. insulin). As shown in Figure 6b, starved cells display long and densely packed stress fibers (visualized with phalloidin). In contrast, starved cells treated with 10 μM PHDM displayed shorter and less densely packed stress fibers. At the higher concentration of 50 μM actin stress fibers disappear nearly completely. These observations provide further evidence that PHDM is capable of binding to $PI(4,5)P_2$ *in vivo*, which will then in turn affect cellular function.

PHDM decreases the amount of mitochondria

We recently demonstrated that mitochondrial destiny is controlled by $PI(4,5)P_2$ (*34*). In particular, targeting the PLC-δ1 PH domain towards the outer membrane of mitochondria caused a gradual fragmentation in the mitochondrial network and ultimately a loss of

mitochondria, which could be partially rescued by PKC. This implies that a $PI(4,5)P_2$-PLC-PKC dependent process is controlling the survival of mitochondria, which can be overcome by masking the available $PI(4,5)P_2$ on the outer membrane of mitochondria. A chemical mimetic of the PLC-δ1 PH domain should therefore cause the loss of mitochondria, which indeed was observed when cells were treated with 50 μM PHDM (Figure 6c).

Taking all these observations together, it is evident that PHDM is a potent chemical receptor mimicking the PLC-δ1 PH domain with respect to lipid binding. Our *in vitro* studies reveal that PHDM binds $PI(4,5)P_2$ selectively and with high affinity. Until now, $PI(4,5)P_2$-binding molecules, such as poly-lysine (*35*) and neomycin (*36*) have been used to reduce endogenous $PI(4,5)P_2$ levels. However, both poly-lysine and neomycin lack specificity since both bind $PI(4,5)P_2$ and other polar lipids (e.g. PtdSer) via electrostatic interactions (*14*). Langeland et al. demonstrated via binding experiments of column-immobilized poly-lysine and neomycin, that both compounds bind to phosphatidylserine, phosphatidylinositol and phosphatidylinositol monophosphate (*37*). These two binding agents are therefore not ideal to study $PI(4,5)P_2$-dependent functions. In contrast, PHDM displays high specificity for $PI(4,5)P_2$, offering a valuable and unprecedented alternative to these tools. Much of its specificity and potency can most likely be attributed to the well documented ability of boronic acid to form strong covalent bonds with *cis*-1,2-diols – such as the *cis*-1,2-diol present in $PI(4,5)P_2$ (*38*). This type of interaction has been exploited in the past to separate PI(3)P from PI(4)P in thin layer chromatography(*39*). Since all 3-phosphorylated inositol lipids lack the *cis*-diol (2' and 3' hydroxyls of the inositol; see figure 1a), PHDM cannot bind any of these lipids with sufficient affinity. However, removing a phosphate on the inositol head group will weaken the interaction with the urea moiety of PHDM, which may explain why PHDM favors $PI(4,5)P_2$ over PI(4)P and PI(5)P, where the *cis*-diols are available for binding.

We have demonstrated that the high specificity of PHDM enable us to employ it as a research tool to study $PI(4,5)P_2$-dependent processes in the cellular environment. Currently, altering cellular $PI(4,5)P_2$ levels requires the use of chemical dimerizers (*40-43*), biological lipid recognition domains or lipid metabolizing enzymes, which are prone to interference by protein-protein interactions. In addition, response times are subject to biological restrains, since the cell has to express sufficient amounts of protein prior to any observable effects. In contrast, employing PHDM allows to disturb $PI(4,5)P_2$ levels in a dose-dependent and dynamic manner.

As a number of recent reviews pointed out, $PI(4,5)P_2$ might be a potential therapeutic target in numerous human diseases (*6, 44*). Since the level of $PI(4,5)P_2$ is tightly controlled by phosphoinositide kinases, phospholipases and phosphatases, they have been the most obvious targets to manipulate the level of $PI(4,5)P_2$.

Chemical biological research tools, like PHDM, which are custom-designed to target a substrate (as opposed to a protein), could unlock great potential for modulation of biological functions and could well gain the same momentum in drug discovery programs in future years as protein-targeted molecules. One particular disease that could benefit in the future from PHDM is the Lowe syndrome caused by the loss of the OCRL $PI(4,5)P_2$ 5-phosphatase, which in turn results in elevated $PI(4,5)P_2$ levels (*43*).

METHODS

Chemical synthesis

Synthesis of compound 2: Mono-Boc protected diamine **1** (0.92 g, 3.9 mmol, 1 equiv), 2-formylphenylboronic acid (0.58 g, 3.9 mmol, 1 equiv) and 3 Å molecular sieves were transferred to a round-bottom flask, which was sealed and purged with nitrogen. Anhydrous MeOH (18.4 mL) was added followed by triethylamine (5.43 mL, 39 mmol, 10 equiv), and the mixture was vigorously stirred at room temperature (RT) for 2 h, then at 40 ^{o}C for another 2h. It was then allowed to cool down to RT and after addition of solid $NaBH_4$ (0.44 g, 11.7 mmol, 3 equiv) it was stirred at RT for 2 h. The mixture was filtered through celite, concentrated under vacuum, and treated with triethylorthoformate (1.95 mL, 11.7 mmol, 3 equiv) and a few drops of glacial acetic acid for 5–6 h at RT. The solvent was finally removed under vacuum and the solid was washed with petroleum ether, water and petroleum ether again, and left to dry first on the filter and then on a high vacuum line. This process afforded the desired compound **2** in 89% yield (1.28 g, 3.47 mmol) as a white solid. ^{1}H-NMR (CD_3OD, 3.31 ppm) δ(ppm): 1.46 (9H, singlet), 3.86 (2H, singlet), 3.97 (2H, singlet), 4.25 (2H, singlet), 7.07 (1H, doublet, J=6.5 Hz), 7.19 (2H, m), 7.34 (2H, doublet, J=7.9 Hz), 7.42 (2H, doublet, J=7.9 Hz), 7.48 (1H, doublet, J=6.5 Hz). ^{13}C-NMR (CD_3OD, 49.00 ppm)-δ(ppm): 28.79, 44.73, 51.88, 54.13, 80.21, 124.25, 127.67, 128.34, 128.66, 129.79, 130.95, 131.62, 134.86, 141.42, 142.36, 158.54. LC-MS (ESI^+): Calculated (M+H) 371.21 a.m.u.; found 371.21 a.m.u.

Synthesis of compound 3: Compound **2** (0.24 g, 0.65 mmol, 1 equiv) was transferred to a round-bottom flask, which was sealed and purged with nitrogen. Anhydrous CH_2Cl_2 (65 mL) was added, and the mixture was cooled to –78 ^{o}C before dropwise addition of TFA (3 mL, 40 mmol, 61.5 equiv). The mixture was vigorously stirred at –78 ^{o}C for 1 h, then the temperature was allowed to slowly rise to RT over 5 h. The solvent was removed under vacuum to give

compound **3** as a colorless oil, which was further dried on high vacuum for 24 h and used directly in the synthesis of **4** (see below). ^{1}H-NMR indicated 100% boc deprotection, and ^{13}C and ^{19}F-NMR suggested the presence of some remaining TFA which, based on the obtained mass of 0.545 g, was determined to be 5 equiv. of TFA per molecule of **3**. ^{1}H-NMR (CD_3OD, 3.31 ppm) δ(ppm): 4.17 (2H, singlet), 4.30 (4H, singlet), 7.43 (3H, broad singlet), 7.59 (4H, broad singlet), 7.80 (1H, broad singlet).^{13}C-NMR (CD_3OD, 49.00 ppm)-δ(ppm): 43.73, 51.63, 52.81, 116.75 (TFA CF_3, quartet), 129.88, 130.79, 131.64, 131.82, 131.99, 132.45, 133.27, 135.87, 136.70, 136.90, 167.09 (TFA carboxylate). LC-MS (ESI^+): Calculated (M+H) 271.16 a.m.u.; found 271.16 a.m.u.

Synthesis of compound 4: Compound **3**, as its TFA salt (0.44 g, 0.52 mmol, 2 equiv), was transferred to a round-bottom flask, which was sealed and purged with nitrogen. Anhydrous DMF (6 mL) was added, followed by addition of triethylamine (3.62 mL, 26 mmol, 100equiv) at RT, and stirring for 10 min. The excess triethylamine was used to neutralize residual TFA from the previous step. A solution of 4,4'-methylenebis(phenyl isocyanate) (0.065 g, 0.26 mmol, 1 equiv) in 1.5 mL DMF was added dropwise and the reaction was allowed to stir at RT for 48 h. The mixture was then concentrated under vacuum and the product was precipitated out of solution as a white solid by addition of water. It was filtered and washed extensively with water and CH_2Cl_2. This process afforded 60% of compound **4** (0.123 g, 0.16 mmol). ^{1}H-NMR (CD_3OD, 3.31 ppm) δ(ppm): 3.85 (2H, singlet), 3.86 (4H, singlet), 3.97 (4H, singlet), 4.40 (4H, singlet), 7.08 (6H, multiplet), 7.17 (4H, multiplet), 7.26 (4H, doublet, J=8.6 Hz), 7.38 (4H, doublet, J=8.2 Hz), 7.43 (4H, doublet, J=8.2 Hz), 7.47 (2H, multiplet).^{13}C-NMR (CD_3OD, 49.00 ppm)-δ(ppm): 41.47, 44.18, 51.85, 54.15, 120.61, 127.67, 128.30, 128.72, 129.82, 130.18, 131.03, 134.96, 137.25, 138.75, 141.61, 142.26, 145.74, 148.96, 158.36. LC-MS (ESI^+): Calculated (M+H) 791.39 a.m.u.; found 791.40

a.m.u. IR (cm^{-1}): 757, 813, 1235, 1309, 1361, 1414, 1514, 1544, 1600, 1660. Elemental analyses: calculated for $C_{45}H_{48}B_2N_6O_6 \cdot ½H_2O$: C, 67.6; H, 6.2; N, 10.5; found: C, 67.7; H, 6.1; N, 9.9.

Biological methods

Protein expression and purification

All lipid-binding domains, OCRL, SKIP, SopB as well as PTEN were expressed and purified as GST-fusion protein. Protein expression was induced in the *E. coli* strain DH5α for 24 h using 1 mM IPTG at 23° C. After growth the cells were harvested and the pellet was stored at –20°C. The harvested cells were resuspended in lysis buffer containing 50 mM Tris (pH 7.4), 1% Triton X-100, 10 mM benzamidine hydrochloride, 100 µg mL^{-1} soybean trypsin inhibitor, 1 mM 4-(2-Aminoethyl)benzenesulfonyl fluoride hydrochloride and 2 mM DTT. Lysozyme was added to the cell suspension at a concentration of 2 mg m^{-1} L and stirred for 1 h at 4°C. Lysis was performed by sonication, followed by centrifugation at 18000 g for 1 h at 4°C. The supernatant was loaded onto a glutathione sepharose column, pre-equilibrated with 50 mM Tris (pH 7.4), 140 mM NaCl and 2.7 mM KCl. After loading, the column was washed twice with 50 mM Tris (pH 7.4), 140 mM NaCl, 2.7 mM KCl and 2 mM DTT. Another two washes were performed using the same buffer with 500 mM NaCl. The GST-tagged protein was eluted using 20 mM glutathione in 50 mM Tris (pH 7.4), 250 mM NaCl, 20% (v/v) glycerol and 2 mM DTT. Protein integrity was confirmed by Western blotting using GST-antibody. Protein concentration was determined using Bradford assay.

Protein-lipid overlay assay

Inositol phospholipids were pre-incubated with increasing concentration of PHDM or solvent control for 20 min. 50 pmol of inositol-phospholipid was spotted onto a nitrocellulose membrane followed by blocking with 0.25% (w/v) fatty-acid free bovine serum albumin (BSA) in 50 mM TRIS buffer, pH 7.4. Membrane was washed 3 times with 50 mM TRIS pH 7.4 containing 150 nM sodium chloride and 0.1% (v/v) Tween 20 (TBST) for 5 min each. Membranes were then incubated with the corresponding lipid-binding domain in blocking buffer. The concentrations of lipid-binding domains were optimized to insure a dose-dependent detection of bound lipid. The following concentrations of lipid-binding domains were used: 25 nM PLC-δ1 PH domain, 5 nM FYVE domain, 50 nM FAPP1 domain, 25 nM Akt PH domain and 50 nM GRP1 PH domain. After washing with TBST for 1 hour bound PH domain was visualized using a GST-antibody and horseradish-peroxidase-conjugated secondary antibody with washing of 1 hour in TBST in between. Membrane was then probe using western blotting detection reagent.

Phosphatase enzyme assay with inositol phospholipid substrates

Inositol phospholipids were presented as mixed micelles with octyl glucoside. Therefore, lipids were sonicated with 1% (v/v) octyl glucoside in assay buffer (100 mM Tris, pH 7.4) for 10 min and added to the assay with a final concentration of 0.25% (v/v) octyl glucoside. Phosphatase activities were measured in 100 mM Tris, pH 7.4 and 4 mM $MgCl_2$ at 37˚C for 30 min. Reactions were terminated after 30 min by adding 2.25 volume of color reagent (5 mM malachite green oxalate, 17 mM ammonium heptamolybdate, 77 mM bismuth citrate and 1.7 M HCl) to quantify amount of phosphate release. The mixture was allowed to develop for 10 min at RT, and the absorbance was read at 625 nm. All enzyme assays were performed in a 96-well microtiter plate.

Phosphatase enzyme assay with OMFP as substrate

3-*O*-Methylfluorescein phosphate cyclohexylammonium salt (OMFP) was dissolved into anhydrous DMSO to a concentration of 20 mM and then further diluted with 1 % (v/v) DMSO to the tested concentrations. Assays were performed in 100 mM TRIS (pH 7.4) containing 4 mM $MgCl_2$. Reactions were initialized by adding OMFP to the enzyme-buffer mixture. The hydrolysis of OMFP to OMF was monitored by measuring the change of fluorescence units in a 96-well microtiter plate (excitation at 485 nm and emission at 525 nm) using a Varian fluorescence spectrophotometer.

Cytotoxicity assay

NIH 3T3 cells were seeded into a 96-well plate at a concentration of ~8,000 cells per well and incubated at 37 °C for 16 h. Cells were treated with PHDM at concentrations between 5 μM and 50 μM for 2 h or 16 h, respectively at 37 °C (total volume of 100 μL). After 2 h or 16 h, 20 μL of a 5 mg mL^{-1} MTT solution was added to each well and the mixture was incubated for a further 4 h at 37 °C. The media were removed carefully, 150 μL of 4 mM HCl in isopropyl alcohol was added to each well, and the mixture was incubated at room temperature for 15 min on an orbital shaker. The formation of formazan by viable cells was measured using a spectrophotometer at 590 nm.

Detection of cellular $PI(4,5)P_2$ via immunofluorescence

Detection of cellular $PI(4,5)P_2$ was performed according to the methods previously described with some modifications(*45*). NIH 3T3 mouse fibroblast were grown in Dulbecco's modified Eagle's medium (DMEM) supplemented with 10% bovine calf serum in an atmosphere of 5% CO_2 at 37˚C. Cells were seeded onto glass coverslips in a 24-well plate and starved overnight in serum-free DMEM. Cells were incubated with PHDM or DMSO and fixed with 4 % paraformaldehyde (PFA) for 15 min at RT. After 3 washes with 50 mM ammonium chloride in phosphate buffer saline (PBS), plate was chilled on ice for 20 min, prior to

permeabilization with 0.5% (w/v) saponin in PBS for 30 min. Coverslips were block with 3% fatty acid free bovine serum albumin (BSA), followed by 3 washes with NH_4Cl/PBS. 100 nM of GST-tagged PLC-δ1 PH domain in blocking bluffer were added to the cells and incubate for 1 hour on ice. Cells were washed three times with NH_4Cl/PBS and an Alexa 488-conjugated GST-specific antibody was added and incubated for 1 hour at RT. After 3 washes with PBS, cells were fixed with 2% PFA for 10 min at RT. Cells were washed 3 times with PBS and then treated with 300 nM 4',6-diamidino-2-phenylindole (DAPI) for nuclear counterstaining. Thoroughly washed coverslips were mounted onto glass slides using Mowiol supplemented with 0.6% (w/v) 1,4-diazabicyclo-[2.2.2]octane. Fluorescence microscopy was performed using a Nikon TE 2000 fluorescence microscope. Filters used in the fluorescence experiments were band pass for DAPI, FITC and TRITC with excitation wavelength of (nm) 340–380, 465–495 and 540–580, respectively, and with emission wavelength of (nm) 435–485, 515–555 and 572–605, respectively. Images were digitally acquired with a CCD camera (Hamamatsu) for each fluorophore separately and processed using IPLab software v 3.65a and ImageJ.

Transferrin uptake assay, detection of actin stress fibers and mitochondria staining

NIH 3T3 cells were grown on coverslips in 10% bovine calf serum DMEM for 24 h. Cells were incubated with compound PHDM at concentrations indicated or solvent control respectively for 30 min in serum free DMEM. Alexa 488-human transferrin conjugate was added in serum free DMEM at a final concentration of 5 μg ml^{-1} and any excess was washed away with acidic PBS and subsequently neutral PBS (after 15min) . For stress fibers detection cells were incubated with FITC-conjugated phalloidin for 1 hour at RT. For mitochondria staining, cells were treated with MitoTracker Red 580 (Invitrogen) according to manufacturer's protocol. Cells were PFA fixed and nuclei were DAPI stained. The coverslips

were mounted in MOWIOL mounting medium and subjected to fluorescence microscopy as described above.

Fluorescence time-lapse microscopy

NIH 3T3 cells transfected with GFP-PLC-δ1 PH domain were observed under a Nikon TE 2000 fluorescence microscope using a 100× Fluor oil lens. Images were taken every 1 min after addition of PHDM or vehicle control.

Acknowledgement

This work was supported by the Lowe Syndrome Trust (UK), the Leverhulme Trust (UK) and the Engineering and Physical Sciences Research Council (EPSRC, UK).

REFERENCES

1. Katso, R., Okkenhaug, K., Ahmadi, K., White, S., Timms, J., and Waterfield, M. D. (2001) CELLULAR FUNCTION OF PHOSPHOINOSITIDE 3-KINASES: Implications for Development, Immunity, Homeostasis, and Cancer, *Annual Review of Cell and Developmental Biology 17*, 615-675.
2. Berridge, M. J., and Irvine, R. F. (1984) Inositol Trisphosphate, a Novel 2nd Messenger in Cellular Signal Transduction, *Nature 312*, 315-321.
3. Sakisaka, T., Itoh, T., Miura, K., and Takenawa, T. (1997) Phosphatidylinositol 4,5-bisphosphate phosphatase regulates the rearrangement of actin filaments, *Mol. Cell. Biol. 17*, 3841-3849.
4. Raucher, D., Stauffer, T., Chen, W., Shen, K., Guo, S., York, J. D., Sheetz, M. P., and Meyer, T. (2000) Phosphatidylinositol 4,5-Bisphosphate Functions as a Second Messenger that Regulates Cytoskeleton-Plasma Membrane Adhesion, *Cell 100*, 221-228.
5. Hilgemann, D. W., Feng, S., and Nasuhoglu, C. (2001) The Complex and Intriguing Lives of PIP2 with Ion Channels and Transporters, *Sci. STKE 2001*, re19-.

6. McCrea, H. J., and De Camilli, P. (2009) Mutations in Phosphoinositide Metabolizing Enzymes and Human Disease, *Physiology 24*, 8-16.
7. Wenk, M. R., Lucast, L., Di Paolo, G., Romanelli, A. J., Suchy, S. F., Nussbaum, R. L., Cline, G. W., Shulman, G. I., McMurray, W., and De Camilli, P. (2003) Phosphoinositide profiling in complex lipid mixtures using electrospray ionization mass spectrometry, *Nat Biotech 21*, 813-817.
8. Fruman, D. A., Meyers, R. E., and Cantley, L. C. (1998) PHOSPHOINOSITIDE KINASES, *Annual Review of Biochemistry 67*, 481-507.
9. Blero, D., Payrastre, B., Schurmans, S., and Erneux, C. (2007) Phosphoinositide phosphatases in a network of signalling reactions, *Pflügers Archiv European Journal of Physiology 455*, 31-44.
10. McLaughlin, S., Wang, J., Gambhir, A., and Murray, D. (2002) PIP2 AND PROTEINS: Interactions, Organization, and Information Flow, *Annual Review of Biophysics and Biomolecular Structure 31*, 151-175.
11. Garcia, P., Gupta, R., Shah, S., Morris, A. J., Rudge, S. A., Scarlata, S., Petrova, V., McLaughlin, S., and Rebecchi, M. J. (1995) The pleckstrin homology domain of phospholipase C-.delta.1 binds with high affinity to phosphatidylinositol 4,5-bisphosphate in bilayer membranes, *Biochemistry 34*, 16228-16234.
12. Rohacs, T., and Nilius, B. (2007) Regulation of transient receptor potential (TRP) channels by phosphoinositides, *Pflügers Archiv European Journal of Physiology 455*, 157-168.
13. Gabev, E., Kasianowicz, J., Abbott, T., and McLaughlin, S. (1989) Binding of neomycin to phosphatidylinositol 4,5-biphosphate (PIP2), *Biochimica et Biophysica Acta (BBA) - Biomembranes 979*, 105-112.
14. Palmer, F. B. (1981) Chromatography of acidic phospholipids on immobilized neomycin, *Journal of Lipid Research 22*, 1296-1300.
15. Amendola, V., Fabbrizzi, L., and Mosca, L. (2010) Anion recognition by hydrogen bonding: Urea-based receptors, *Chemical Society Reviews 39*, 3889-3915.
16. Gale, P. A. (2011) Anion receptor chemistry, *Chemical Communications (Cambridge, United Kingdom) 47*, 82-86.
17. Kang, S. O., Begum, R. A., and Bowmna-James, K. (2006) Amide-based ligands for anion coordination, *Angewandte Chemie, International Edition 45*, 7882-7894.
18. Katayev, E. A., Ustynyuk, Y. A., and Sessler, J. L. (2006) Receptors for tetrahedral oxyanions, *Coordination Chemistry Reviews 250*, 3004-3037.
19. Fossey, J. S., and James, T. D. (2009) Boronic acid based modular fluorescent saccharide sensors, *Reviews in Fluorescence 4*, 103-118.
20. Nishiyabu, R., Kubo, Y., James, T. D., and Fossey, J. S. (2011) Boronic acid building blocks: tools for self assembly, *Chemical Communications (Cambridge, United Kingdom) 47*, 1124-1150.
21. Gillooly, D. J., Morrow, I. C., Lindsay, M., Gould, R., Bryant, N. J., Gaullier, J.-M., Parton, R. G., and Stenmark, H. (2000) Localization of phosphatidylinositol 3-phosphate in yeast and mammalian cells, *EMBO J 19*, 4577-4588.
22. Norris, F. A., Wilson, M. P., Wallis, T. S., Galyov, E. E., and Majerus, P. W. (1998) SopB, a protein required for virulence of Salmonella dublin, is an inositol phosphate phosphatase, *Proceedings of the National Academy of Sciences of the United States of America 95*, 14057-14059.
23. Faucherre, A. l., Desbois, P., Nagano, F., Satre, V. r., Lunardi, J. l., Gacon, G. r., and Dorseuil, O. (2005) Lowe syndrome protein Ocrl1 is translocated to membrane ruffles upon Rac GTPase activation: a new perspective on Lowe syndrome pathophysiology, *Human Molecular Genetics 14*, 1441-1448.

24. Ijuin, T., Mochizuki, Y., Fukami, K., Funaki, M., Asano, T., and Takenawa, T. (2000) Identification and Characterization of a Novel Inositol Polyphosphate 5-Phosphatase, *Journal of Biological Chemistry 275*, 10870-10875.
25. Schmid, A. C., Wise, H. M., Mitchell, C. A., Nussbaum, R., and Woscholski, R. (2004) Type II phosphoinositide 5-phosphatases have unique sensitivities towards fatty acid composition and head group phosphorylation, *FEBS Letters 576*, 9-13.
26. Mallo, G. V., Espina, M., Smith, A. C., Terebiznik, M. R., Aleman, A., Finlay, B. B., Rameh, L. E., Grinstein, S., and Brumell, J. H. (2008) SopB promotes phosphatidylinositol 3-phosphate formation on Salmonella vacuoles by recruiting Rab5 and Vps34, *The Journal of cell biology 182*, 741-752.
27. Lemmon, M. A., and Ferguson, K. M. (2000) Signal-dependent membrane targeting by pleckstrin homology (PH) domains, *Biochem. J. 350*, 1-18.
28. Maehama, T., and Dixon, J. E. (1998) The Tumor Suppressor, PTEN/MMAC1, Dephosphorylates the Lipid Second Messenger, Phosphatidylinositol 3,4,5-Trisphosphate, *J. Biol. Chem. 273*, 13375-13378.
29. Steele-Mortimer, O., Knodler, L. A., Marcus, S. L., Scheid, M. P., Goh, B., Pfeifer, C. G., Duronio, V., and Finlay, B. B. (2000) Activation of Akt/Protein Kinase B in Epithelial Cells by theSalmonella typhimurium Effector SigD, *Journal of Biological Chemistry 275*, 37718-37724.
30. Dowler, S., Kular, G., and Alessi, D. R. (2002) Protein Lipid Overlay Assay, *Sci. STKE 2002*, pl6-.
31. Mosmann, T. (1983) Rapid colorimetric assay for cellular growth and survival: Application to proliferation and cytotoxicity assays, *Journal of Immunological Methods 65*, 55-63.
32. Watt, S. A., Kular, G., Fleming, I. N., Downes, C. P., and Lucocq, J. M. (2002) Subcellular localization of phosphatidylinositol 4,5-bisphosphate using the pleckstrin homology domain of phospholipase C delta1, *Biochem. J. 363*, 657-666.
33. Kim, S., Kim, H., Chang, B., Ahn, N., Hwang, S., Di Paolo, G., and Chang, S. (2006) Regulation of transferrin recycling kinetics by PtdIns[4,5]P2 availability, *FASEB J. 20*, 2399-2401.
34. Rosivatz, E., and Woscholski, R. Removal or masking of phosphatidylinositol(4,5)bisphosphate from the outer mitochondrial membrane causes mitochondrial fragmentation, *Cellular Signalling 23*, 478-486.
35. Zhang, H., Craciun, L. C., Mirshahi, T., Rohács, T., Lopes, C. M. B., Jin, T., and Logothetis, D. E. (2003) PIP2 Activates KCNQ Channels, and Its Hydrolysis Underlies Receptor-Mediated Inhibition of M Currents, *Neuron 37*, 963-975.
36. Schacht, J. (1976) INHIBITION BY NEOMYCIN OF POLYPHOSPHOINOSITIDE TURNOVER IN SUBCELLULAR FRACTIONS OF GUINEA-PIG CEREBRAL CORTEX IN VITRO, *Journal of Neurochemistry 27*, 1119-1124.
37. Langeland, N., Moore, L. J., Holmsen, H., and Haarr, L. (1988) Interaction of Polylysine with the Cellular Receptor for Herpes Simplex Virus Type 1, *J Gen Virol 69*, 1137-1145.
38. Bosch, L., Fyles, T., and James, T. D. (2004) Binary and ternary phenylboronic acid complexes with saccharides and Lewis bases, *Tetrahedron 60*, 11175-11190.
39. Walsh, J. P., Caldwell, K. K., and Majerus, P. W. (1991) Formation of phosphatidylinositol 3-phosphate by isomerization from phosphatidylinositol 4-phosphate, *Proceedings of the National Academy of Sciences 88*, 9184-9187.
40. Fili, N., Calleja, V., Woscholski, R., Parker, P., and Larijani, B. (2006) Compartmental signal modulation: Endosomal phosphatidylinositol 3-phosphate controls endosome morphology and selective cargo sorting, *Proceedings of the National Academy of Sciences 103*, 15473.
41. Varnai, P., Thyagarajan, B., Rohacs, T., and Balla, T. (2006) Rapidly inducible changes in phosphatidylinositol 4,5-bisphosphate levels influence multiple regulatory functions of the lipid in intact living cells, *The Journal of cell biology 175*, 377-382.
42. Zoncu, R., Perera, R. M., Sebastian, R., Nakatsu, F., Chen, H., Balla, T., Ayala, G., Toomre, D., and De Camilli, P. V. (2007) Loss of endocytic clathrin-coated pits upon acute depletion of

phosphatidylinositol 4,5-bisphosphate, *Proceedings of the National Academy of Sciences 104*, 3793-3798.
43. Attree, O., Olivos, I. M., Okabe, I., Bailey, L. C., Nelson, D. L., Lewis, R. A., McLnnes, R. R., and Nussbaum, R. L. (1992) The Lowe's oculocerebrorenal syndrome gene encodes a protein highly homologous to inositol polyphosphate-5-phosphatase, *Nature 358*, 239-242.
44. Im, E., and Kazlauskas, A. (2007) PtdIns-4,5-P2 as a potential therapeutic target for pathologic angiogenesis, *Expert Opinion on Therapeutic Targets 11*, 443-451.
45. Hammond, G. R. V., Schiavo, G., and Irvine, R. F. (2009) Immunocytochemical techniques reveal multiple, distinct cellular pools of PtdIns4P and PtdIns(4,5)P2, *Biochemical Journal 422*, 23-35.

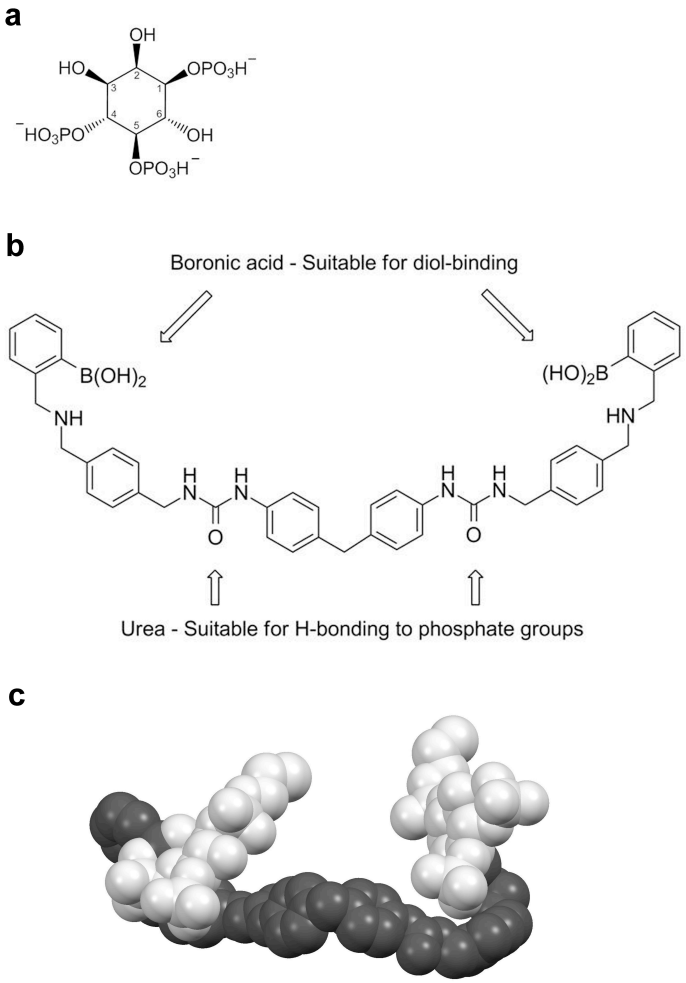

Figure 1. (a) Chemical structure of D-myo-inostiol (1,4,5). (b) Chemical structure of receptor (PHDM) with diol and phosphate-binding groups; a large and relatively rigid spacer allows for two separate PI(4,5)P_2 binding pockets to be present in the same molecule. (c) Space-fill computer model of the receptor under study (PHDM) binding two different PI(4,5)P_2 molecules (the receptor is shown in black and the PI(4,5)P_2 molecules in white). Hydrogens have been omitted for clarity; the aliphatic chain attached to PI(4,5)P_2 was substituted for shorter propyl groups to simplify the calculations. Optimization was carried out by molecular mechanics first, MM2 force field, followed by DFT calculations at the B3LYP/6-31G level using Gaussian.

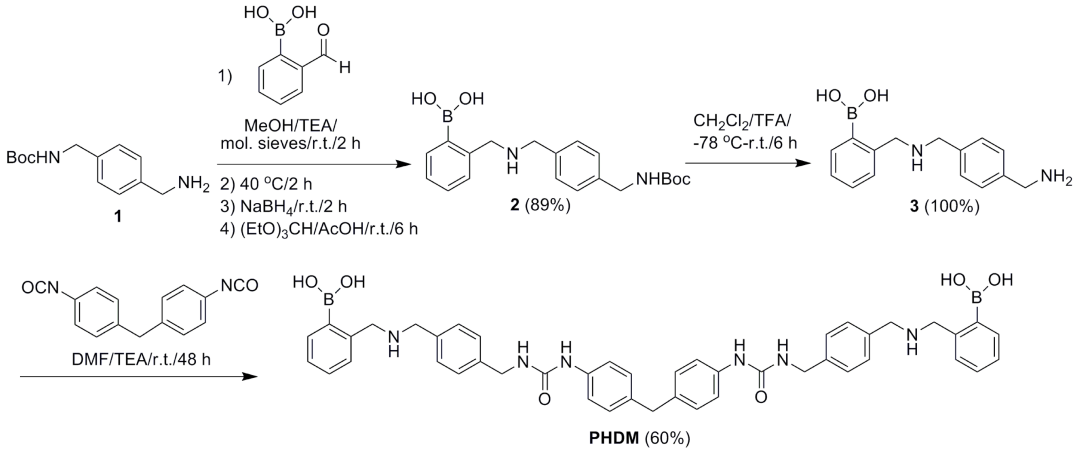

Scheme 1. Reaction scheme for the synthesis of PHDM.

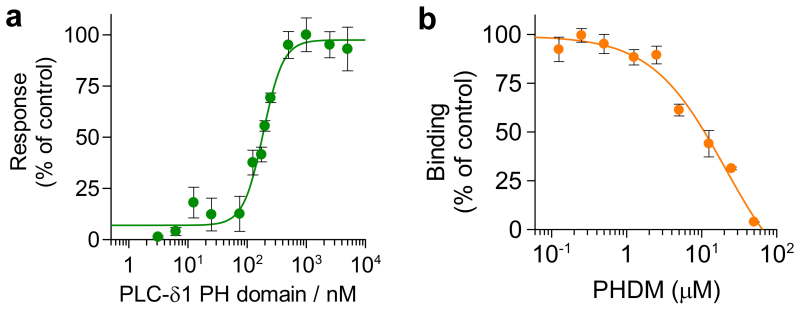

Figure 2. (a) Immobilized PI(4,5)P_2 was assayed in the dependence of PH domain concentration. (b) Competition ELISA for determination of dissociation constant of PHDM. Displacement curve is shown as a function of PHDM concentration. The K_d is determined to be 17.6 ± 10.1 μM. Data presented are the mean ± the standard deviation of at least three independent experiments performed in triplicates (n=3).

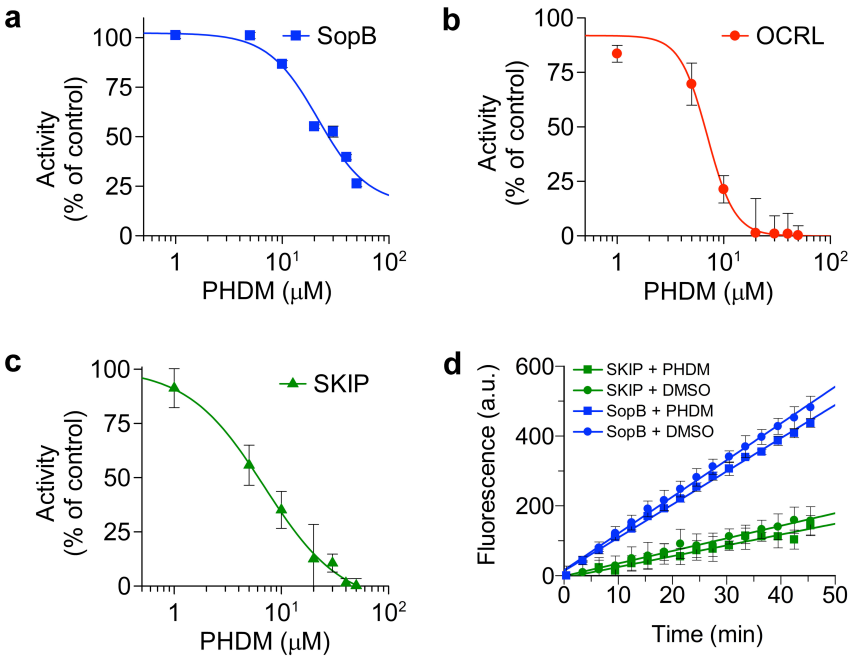

Figures 3. (a–c) PI(4,5)P_2 hydrolyzing phosphatases SopB, OCRL and SKIP were used in dose response studies of compound PHDM. PI(4,5)P_2 was presented in octyl glucoside mixed micelles at a substrate concentration of 20 μM which is around the K_M value reported for these three enzymes (SKIP and OCRL: 23 μM (24), SopB: 28 μM). Phosphatase activity was determined as described earlier (24). The IC50s were determined to be: SopB: 21.6 ± 6.5 μM, OCRL: 7.0 ± 0.6 μM, SKIP: 6.9 ± 0.7 μM. (d) SopB and SKIP in phosphatase assay with artificial substrate 3-O-methylfluorescein phosphate (OMFP) with and without PHDM. PHDM was used at a concentration of 50 μM with 150 μM OMFP substrate. OCRL could not be tested in this manner, since it has no detectable OMFP activity.

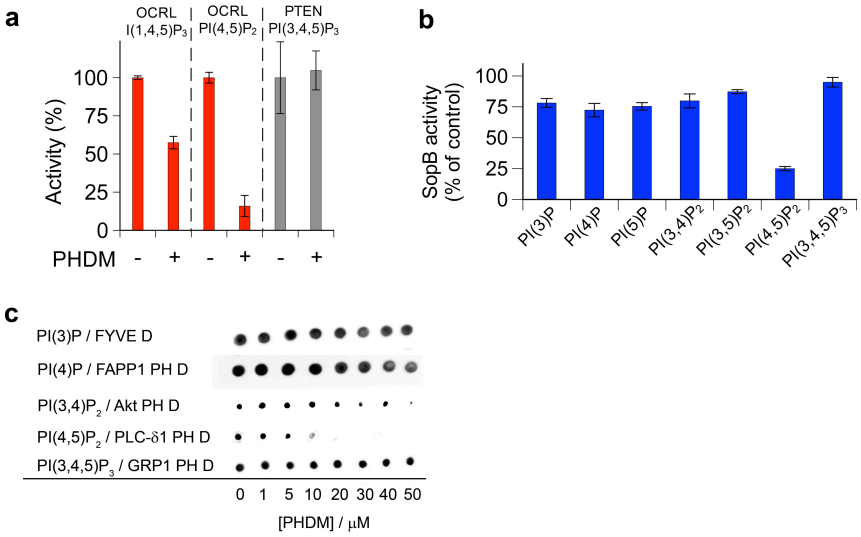

Figure 4 (a) Head group specificity of PHDM studied with OCRL/I(1,4,5)P_3 and PI(4,5)P_2 and PTEN/PI(3,4,5)P_3. The remaining phosphatase activities in the presence of 20 µM PHDM compared to control are shown. All 3 substrates were used at a concentration of 20 µM. (b) Head group specificity of PHDM towards all 7 inositol phospholipids in phosphatase assays with SopB. All tested inositol-phospholipids contain the same fatty acid composition (diC16, palmitoyl) to ensure comparison of PHDM specificity based only on the inositol head group. Lipids were presented in octyl glucoside mixed micelles at concentrations of 20 µM. PHDM was used at 50 µM and the remaining SopB activities are presented as percentage of solvent control (no PHDM). The amount of SopB employed were adjusted for each inositol-phospholipid to ensure similar turnover rates (for details see supplementary figure 2). (c) Protein-lipid overlay assay in the presence of PHDM. Inositol phospholipids were pre-incubated with increasing concentrations of PHDM followed by incubation with GST-tagged lipid-binding domains. Bound domains were visualized with anti-GST and horseradish peroxidase antibodies. Results shown are representative of 3 independent experiments.

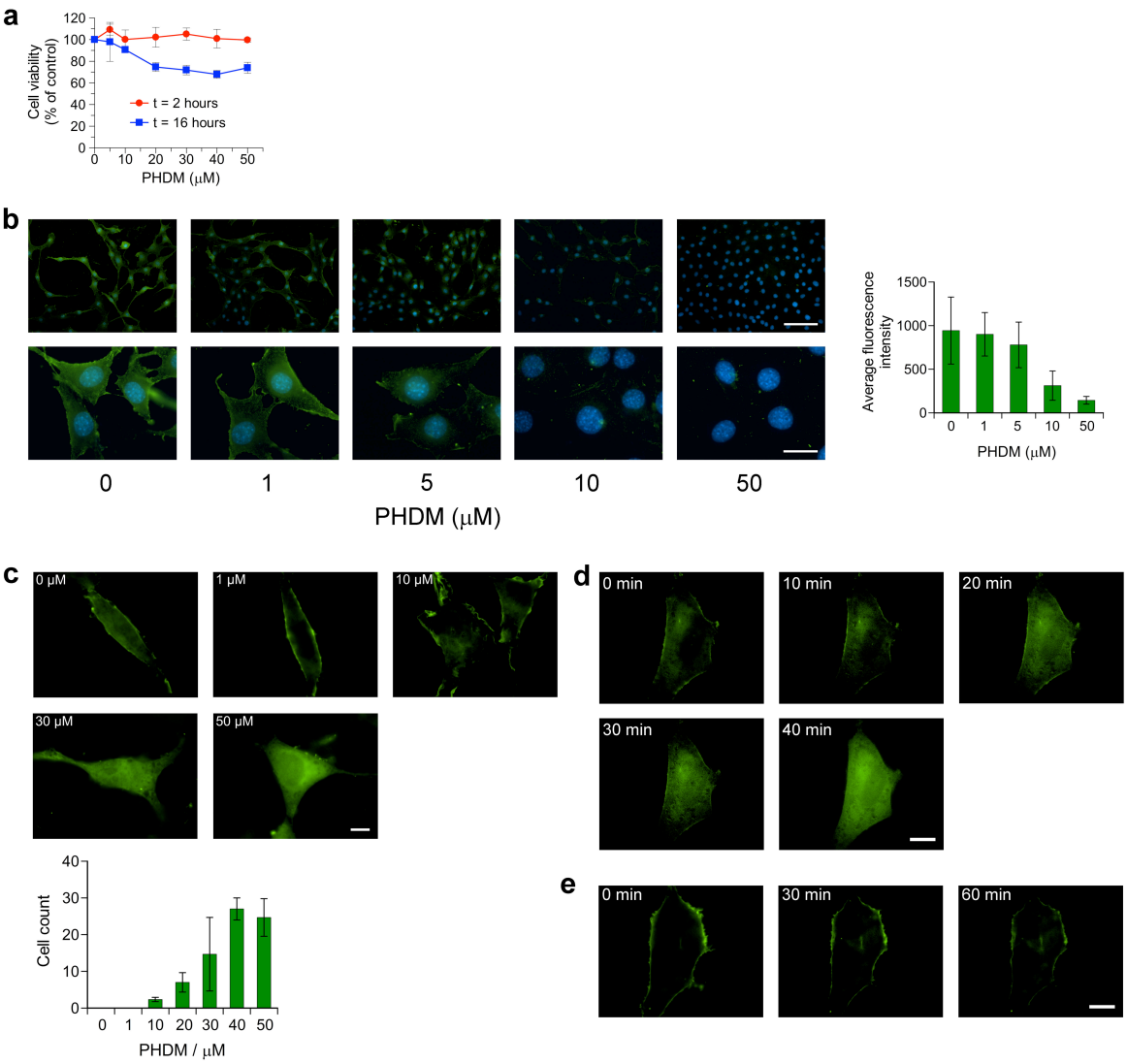

Figure 5. (a) Cytotoxicity of compound PHDM studied using MTT assay. NIH 3T3 cells were incubated with PHDM for 2 h and 16 h at concentrations as indicated. The results are presented as the mean ± the standard deviation of 4 independent experiments performed in triplicates (n = 4). (b) Immunofluorescence of bound PLC-δ1 PH domain in the presence of PHDM. Starved NIH 3T3 fibroblast were treated with concentrations of PHDM as indicated, PFA-fixed and incubated with GST-tagged PLC-δ1 PH domain, followed by incubation with Alexa 488-conjugated GST-specific antibody. Green channel: $PI(4,5)P_2$ staining; blue: DAPI counter stain. Scale bar: top panel: 100 µm; bottom panel: 10 µm. Quantification of bound PH domain from fluorescence imaging using ImageJ are presented in the bar chart on the right side. Data for the quantification was obtained from 6 independent experiments (n = 6)

over a minimum of 180 cells. (c) NIH 3T3 cells were transiently transfected with an expression vector encoding GFP-tagged PLC-δ1 PH domain. 24 hours after tranfection, cells were treated with PHDM at indicated concentrations, PFA-fixed and imaged. Scale bar: 10 μm. Quantification of cells displaying predominantly cytosolic PLC-δ1 PH domain staining are presented in the bar chart on the bottom. Data for the quantification was obtained from 3 independent experiments (n = 3) counting a total of 120 cells. (d) Live cells time-lapse study showing the release of GFP-tagged PLC-δ1 PH domain into the cytosol upon the addition of 40 μM PHDM. Scale bar: 10 μm. Results shown are representative of 8 independent experiments. (e) Control experiment to (d) where the solvent vehicle (DMSO) was added to the cells instead of PHDM. Scale bar: 10 μm. Results shown are representative of 4 independent experiments.

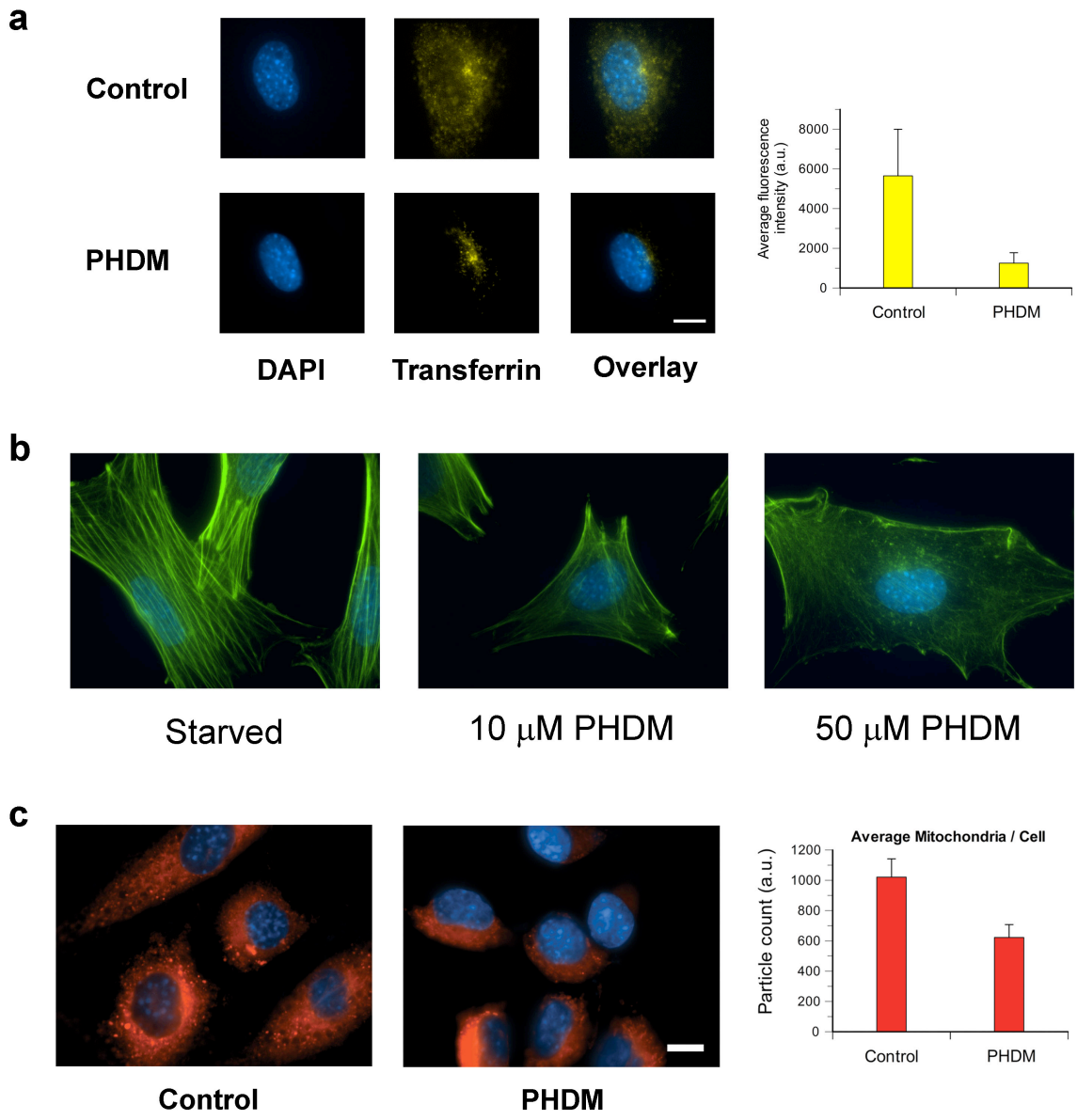

Figure 6. (a) Transferrin uptake in the presence of PHDM. NIH 3T3 cells were treated with 50 μM PHDM or solvent control for 30 min followed by incubation with Alexa 488-conjugated human transferrin for 15 min. Right panel: DAPI (blue); middle panel: transferrin (yellow); left panel:merged images. Scale bar: 10 μm. Quantification of the transferrin uptake assay was performed using ImageJ software (4 independent experiments over a minimum of 20 cells), which is presented in the bar chart on the right side. (b) PHDM induces de-polymerization of stress fibers. Stress fiber formation was monitored with FITC-conjugated phalloidin staining. NIH 3T3 cells were serum starved for 16 hours followed by treatment as indicated. Images shown are representative of 5 independent experiments (n =5). Scale bar: 10 μm. (c) PHDM reduces the size of mitochondria in NIH 3T3 cells. Cells were

treated with 50 μM of PHDM for 30 min followed by staining with MitoTracker probe for 15 min. Cells were fixed, counterstained with DAPI (blue) and examined by fluorescence microscopy. Scale bar: 10 μm. Statistical analysis of mitochondria fluorescence using particle count measurements in randomly chosen fluorescence positive cells (see bar chart on the right side) were performed using ImageJ over a minimum of 280 cells from 3 independent experiments (n=3). Scale bar: 10 μm.

Supporting Information

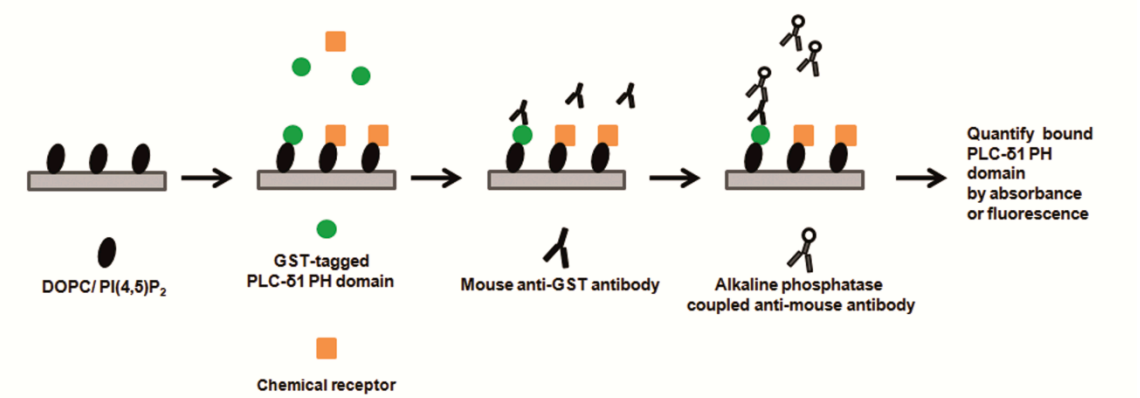

Supplementary Figure 1. Schematic presentation of the ELISA competition assay. Vesicles containing 99% 1,2-dioleoyl-glycero-3-phosphocholine (DOPC) and 1% $PI(4,5)P_2$ were immobilized onto a 96-well microtiterplate. Compound PHDM competes with GST-tagged PLC-δ1 PH domain for binding to $PI(4,5)P_2$. Bound PH domain was quantified using anti-GST antibody and alkaline phosphatase-conjugated secondary antibody. P-nitrophenyl phosphate (substrate) was added and the absorbance at A = 425 nm was recorded.

METHOD

ELISA binding assay

Vesicles containing 99% 1,2-dioleoyl-glycero-3-phosphocholine (DOPC) and 1% $PI(4,5)P_2$ were prepared by sonication for 10 min at RT. A solution containing 0.01 µM lipids were added to a 96-well micro-titer plate and incubated at RT for 2 h. Wells were washes three times with Tris buffer saline (TBS) followed by blocking with 2 % (w/v) goat serum in TBS for 2 h at RT. Wells were washes three times and incubated with either PHDM and/or PH domain for 1 h. After 3 washes with TBS, a GST-antibody (mouse) solution in TBS were added to the wells and incubated at RT for 1 h. Again, wells were washes three times with TBS followed by incubation with an alkaline phosphatase-conjugated anti-mouse antibody at RT for 1 h. Cells were washes three times with TBS and substrate solution containing para-

nitrophenyl phosphate was added. The reaction was monitored with a 96-well ELISA plate reader at an absorbance of A = 405 nm.

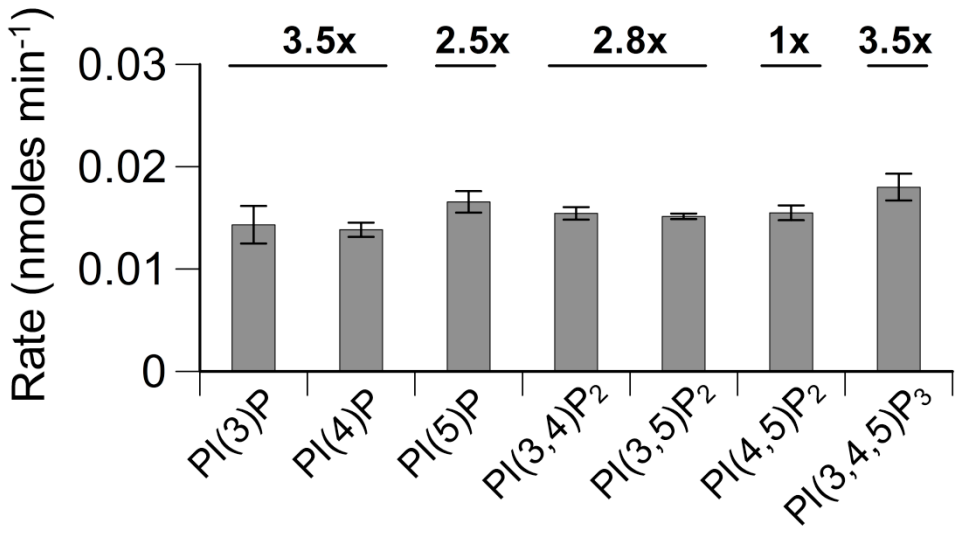

Supplementary Figure 2. SopB amount employed for each lipid in Figure 4b was adjusted in order to achieve similar turnover rates, thus compensating for SopB's substrate specificity differences. The amount of SopB employed for each lipid is given above the bar chart relative to $PI(4,5)P_2$. All data presented are the mean ± the standard deviation of at least three independent experiments performed in triplicates.

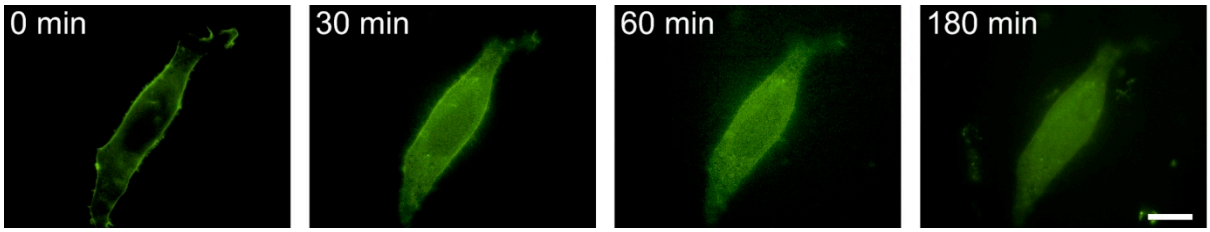

Supplementary Figure 3. Addition of PHDM releases GFP-tagged PLC-δ1 PH domain into the cytosol. NIH 3T3 cells were transiently transfected with an expression vector encoding GFP-tagged PLC-δ1 PH domain. 24 hours after tranfection, cells were treated with PHDM and imaged using time-lapse fluorescence microscopy.